

THE MONTE CARLO METHOD IN THE EMISSION TOMOGRAPHY OF THE TRANSLUCENT ATMOSPHERE

A.E. Bulyshev, L.G. Velikhanova, and N.G. Preobrazhenskii

*F.V. Lukin Scientific-Research
Institute of Physical Problems, Moscow
Received May 29, 1990*

A universal Monte Carlo algorithm has been developed and studied numerically for solving problems associated with the optical tomography of the translucent atmosphere. The algorithm has wide possibilities and makes it possible to solve complicated tomographic problems which are inaccessible to the other methods described in literature. In particular, this method allows one to take account of the spatial structure of the extinction coefficient field, the object need not be convex, requirements for the smoothness of the emission and absorption coefficients are unimportant, the total number of the needed projection data is not great, whereas the noise level may be significant, etc. The results of the calculations are illustrated by specific examples.

In Ref. 1 we described the application of the Monte Carlo method to problems of emission tomography of optically transparent media (the atmosphere in particular). In the case the medium is optically dense, i.e. its absorption coefficient at some chosen frequency, $\mu(r)$, is significantly different from zero, the retrieval of even a two-dimensional field of its emission coefficient $\varepsilon(r)$ from the projective emission data $f(p)$ becomes a considerably more difficult task. Usually this retrieval problem does not admit of an analytical solution. The role of the Monte Carlo method becomes even more important in such circumstances. In particular, heavy computational difficulties are faced when one has to account for the effects of scattering, or for the partial screening of the sensing radiation, when treating non-convex domains of definition of the functions $\varepsilon(r)$ and $\mu(r)$, and in the case when the structure of both the functions ε and μ must be estimated from data on the emission alone, etc.

Neglecting both refraction by the medium and wave effects, we choose as the basis on which to construct our algorithm the Radon exponential transformation,²

$$f(p) = \int_{\infty}^{\infty} \varepsilon(r) \exp \left[- \int_r^p \mu(r') dl' \right] \delta(p - rn) d^2r, \quad (1)$$

Here p is the sighting parameter, $p = pn$, n is a unit vector normal to the sighting line, and δ is the Dirac delta-function. The integration in the exponential is taken from the emitter position r to that of the detector r_D . Below we assume the function $\mu(r)$ to be prescribed, but do not make use of the traditional restriction of a weak spatial dependence of the extinction coefficient ($\mu(r) \approx \text{const}$).²

Let Ω be an arbitrary region, not necessarily convex, covered by a uniform rectangular grid of $N \times N$ nodes. We search for its two-dimensional emission coefficient in the form of a histogram

$$\varepsilon_{ij} = \int_{\Delta_{ij}} \varepsilon(r) d^2r, \quad (2)$$

where the integral is taken over a single grid cell Δ_{ij} . The estimated solution is constructed following a procedure similar to the one employed in Ref. 1. A certain specified "pixel" size h_ε is prescribed, and the value of ε_{ij} is approximated by an integer number of such "pixels" m_{ij}

$$\varepsilon_{ij} \approx m_{ij} h_\varepsilon. \quad (3)$$

The value of h_ε was determined in Ref. 1.

We introduce a Cartesian coordinate system (OXY) within the region Ω , so that its abscissa axis (OX) coincides with the central beam-sum of the first projection. For the sake of definiteness we associate a coordinate axis with the projection: it coincides with the OY axis at the initial moment (the first projection).

Now let us consider the retrieval algorithm in detail.

1. We randomly choose the number of a grid-cell within the retrieval area. If sufficiently reliable *a priori* data on the distribution of the emission coefficient $\varepsilon(x, y)$ in Ω are available, then the cell may be chosen on the basis of such data. In general such a choice is made uniformly over Ω .

2. We place an emitting "pixel" h_ε into the chosen cell (i, j) and estimate its contribution to all

the projections. Our pixel h_ε contributes to every projection, and that contribution is computed according to the integral criterion

$$h_f = h_\varepsilon h, \quad (4)$$

assuming that the projection step coincides with the discretization step h over the region Ω . To improve the statistical properties of the representation, N_0 "quanta" are emitted from the center of the cell (i, j) in the direction of the considered beam-sum.

To account for the spatial dependence of the extinction coefficient, we employ the Neumann technique.³ The mean free path is computed according to the formula

$$\lambda = \frac{\ln \gamma}{\max_{(x, y) \in \Omega} \mu(x, y)}, \quad (5)$$

where γ is a pseudorandom value uniformly distributed over the interval $(0, 1)$. Having progressed to a point a distance λ from the chosen grid cell (i, j) along the sighting line, and having convinced ourselves that the condition $(x', y') \in \Omega$ is satisfied for the new point as well, we play out a random absorption act. If $(x', y') \notin \Omega$ for the new point, we assume the "quantum" not to be absorbed and to be received by the detector. For a point satisfying the condition $(x', y') \in \Omega$ we assume that the "quantum" which has reached it, proceeds to move through the object if

$$\xi \max_{(x, y) \in \Omega} \mu(x, y) \geq \mu(x', y'), \quad (6)$$

Here ξ is a pseudorandom value uniformly distributed over the interval $(0, 1)$. In the latter case we again move along the sighting line the distance λ , etc. Finally, the "quantum" is either absorbed, so that it does not participate in the formation of the projection, or it is registered by the detector. The number of "quanta" received by the detector of the p_k th projection, described by its angle φ_1 , is added to the preceding value $W^{(0)}$

$$W^{(1)}(p_k, \varphi_1) = W^{(0)}(p_k, \varphi_1) + h_\varepsilon \frac{N_1}{N_0}, \quad (7)$$

it is also assumed that at the initial moment $W^{(0)} = 0$ and N_1 is the number of "quanta" hitting the cell (p_k, φ_1) , $k = \bar{1}, \bar{N}$, $l = \bar{1}, \bar{L}$.

3. The values $W^{(1)}(p_k, \varphi_1)$ and $f(p_k, \varphi_1)$ are compared. If $W^{(1)}(p_k, \varphi_1) \leq f(p_k, \varphi_1)$ for every possible k and l , then the step is accepted, the value of ε_{ij} is changed to $\varepsilon_{ij} + h_\varepsilon$, and the projection data set $W^{(0)}$ is replaced by $W^{(1)}$. In the opposite case the step is rejected.

4. We return to position 1. The retrieval procedure is stopped only when the norm of the newly constructed set of projections W deviates from the initial set f by less than some error of the input data,

prescribed *a priori*. In a sense the condition for terminating the computations plays the role of a regularizing procedure.⁴

The step h_f plays the role of a regularization parameter, and it is to be matched with the actual accuracy of the initial data. We now specify the criterion for choosing the value of h_f . The accuracy of the Monte Carlo method is proportional to $M^{-1/2}$, where M is the number of trials.³ Therefore to match our results with projection data which have a noise level of $\eta\%$ (recall that actually we are repeatedly solving the direct problem) we need $M \approx 10^4/\eta$ trials. Determining the average value of f over the projection data

$$\langle f \rangle = \frac{\sum_{k=1}^N \sum_{l=1}^L f(p_k, \varphi_l)}{NL}, \quad (8)$$

we find that

$$h_f = \frac{\langle f \rangle}{M} = \frac{1}{NL} \sum_{k=1}^N \sum_{l=1}^L f(p_k, \varphi_l) \eta \cdot 10^{-4}. \quad (9)$$

Obviously, the "lucky" steps will become rarer and rarer further into the computation as the simulation goes on, since with each succeeding step it becomes more and more difficult to introduce our "pixel" h_ε into the randomly chosen cell (i, j) of the region Ω in such a way as to satisfy all the projections in the process with the newly obtained emission function. If the cell has been chosen erroneously, i.e., if the addition of a new "pixel" into it cannot satisfy all the projections, then the cell should not be considered further on. This feature speeds up the computation quite significantly. In the course of time we thus exclude all the cells of the region Ω from consideration, after which the computation is over.

On the basis of the above-described scheme we have developed a computer software package, and a number of numerical simulations have been run implementing the following closed cycle scheme⁴:

- a) the emission coefficient distribution is generated;
- b) the projections $f(p_k, \varphi_1)$ are found;
- c) a noise factor is introduced into the projection data (for such a noise we employed pseudorandom, uncorrelated, normally distributed values);
- d) the distribution of the emission coefficient $\varepsilon_{ij}^{(0)}$ is retrieved as the corresponding histogram;
- e) the obtained solution is filtered;
- f) the solution is analyzed and graphically presented.

The following two-dimensional functions were chosen as the model ones:

– smooth

$$\varepsilon_1(x, y) = \exp \left[- \left[\frac{x - x_0}{d_0} \right]^2 - \left[\frac{y - y_0}{d_0} \right]^2 \right] +$$

$$+ 0.5 \exp \left[- \left(\frac{x - x_1}{d_1} \right)^2 - \left(\frac{y - y_1}{d_1} \right)^2 \right], \quad (10)$$

— piecewise-constant

$$\epsilon_2(x, y) = \begin{cases} 1 & -0.5 \leq x \leq 0.5; \quad 0.2 \leq y \leq 0.7; \\ 0.5 & -0.5 \leq x \leq 0.5; \quad -0.7 \leq y \leq -0.2; \\ 0 & \text{in the remained region} \end{cases} \quad (11)$$

The extinction coefficient $\mu(x, y)$ was prescribed in the form

$$\mu(x, y) = a + bx^2 + cy. \quad (12)$$

As the region Ω we chose a circle of radius $R_1 = 1$ with its center at the origin.

Another retrieval which we ran over a complicated non-convex region is, apparently, the first one ever to have been conducted

$$\Omega' = \left\{ \{x^2 + y^2 \leq 1\} \cap \{(x + 1)^2 + y^2 \leq 1\} \right\}. \quad (13)$$

One of the advantages of the closed cycle simulations is that comparisons become possible between the constructed and the initial image ($\{\epsilon_{ij}^{(0)}\}$ and $\{\epsilon_{ij}\}$), where $\epsilon_{ij} = \epsilon(x_i + h/2, y_j + h/2)$. Two criteria were employed for such comparative estimates:

$$S = \left(\frac{\sum_{i=1}^N \sum_{j=1}^N (\epsilon_{ij}^{(0)} - \epsilon_{ij})^2}{\sum_{i=1}^N \sum_{j=1}^N \epsilon_{ij}^{(0)2}} \right)^{1/2} \quad (14)$$

(S is sometimes called the rms difference measure), and

$$R = \frac{\sum_{i=1}^N \sum_{j=1}^L |\epsilon_{ij} - \epsilon_{ij}^{(0)}|}{\sum_{i=1}^N \sum_{j=1}^L \epsilon_{ij}}, \quad (15)$$

(R is the normed absolute difference measure). Note that the measure S accounts mostly for the few major errors, and the measure R for the numerous minor ones. Figures 1–4 give some examples of the emission coefficient $\epsilon(x, y)$ retrievals.

Figure 1 depicts the central cross section ($x = 0$) of the model distribution represented by the function

$$\epsilon(x, y) = \exp[-25x^2 - 25(y + 0.5)^2] + 0.5 \exp[-25x^2 - 25(y - 0.5)^2] \quad (16)$$

(see curve 1). The retrieved distribution (curve 2) is characterized by $S = 28\%$ and $R = 24\%$, Figure 2 shows the isolines of the respective tomograms. The retrieval included 16 projections.

Figure 3 gives the central cross section ($x = 0$) of the emission coefficient distribution of the initial model (curve 1) and the retrieval result (curve 2). The distribution $\epsilon(x, y)$ (from the class of the piecewise-constant functions in Eq. (11)) was prescribed over a non-convex domain in Eq. (13). The criterion formulas (14) and (15) give $S = 36\%$ and $R = 28\%$. The number of projections used was $L = 4$. Figure 4 presents the respective tomograms. The retrieval results presented in those figures correspond to heavily noise-loaded initial data (up to 30%). The projection-to-retrieval error transmission coefficient was of the order of unity.

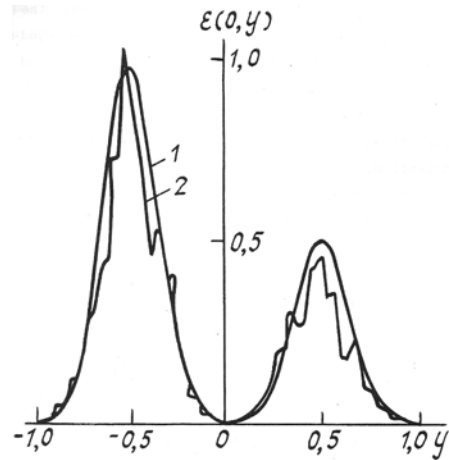


FIG. 1. Curve 1 is a central cross section $\epsilon(0, y)$ of the exact solution (16); curve 2 is the same cross section retrieved by 16 projections.

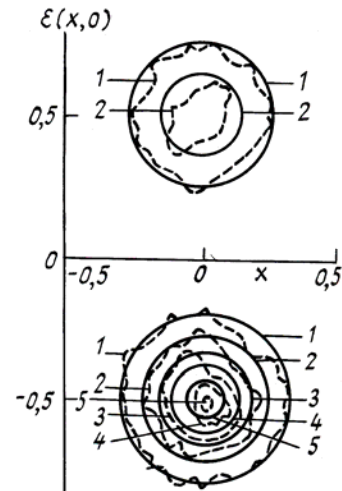


FIG. 2. Distribution isolines of the exact emission coefficient (16) (solid lines) and the retrieved values (dashed lines). Intensity levels: 1 — 0.1, 2 — 0.3, 3 — 0.5, 4 — 0.7, 5 — 0.9.

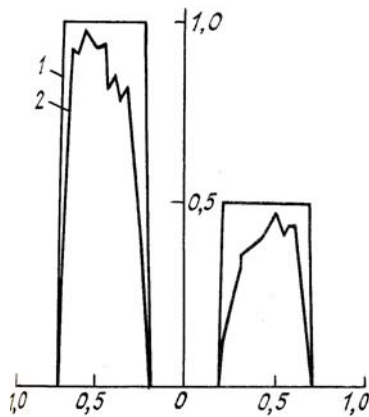


FIG. 3. Curve 1 is the central cross section $\varepsilon(0, y)$ of the exact solution (11); curve 2 is the same cross section retrieved by 4 projections on the non-convex region Ω .

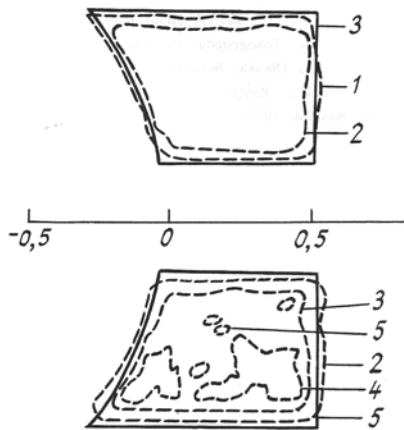


FIG. 4. Isolines of the distribution of the exact emission coefficient (11) (solid lines) and retrieved (dashed lines). Intensity levels: 1 — 0.1; 2 — 0.3; 3 — 0.5; 4 — 0.7; 5 — 0.9.

Our numerical experiments allow us to make the following conclusions:

1. The Monte Carlo retrievals of the emission coefficient may be run for various spatial distributions of the extinction coefficient. The retrieval accuracy is mainly determined by the optical depth of the medium μR_1 . In our computations the optical depth, equal to 8–10, was, already in some sense, critical: qualitative retrievals of the distribution (e.g., tracing out the contours of the emitting areas and determining the average emission level) are still possible beyond that threshold, but quantitative features of the distribution become impossible to identify.

2. The Monte Carlo method of emission coefficient retrieval under conditions of noticeable absorption is quite stable with respect to the projection data errors. A significant part of the computations were conducted at the 20–30% noise level in the projections, however, the error transmission coefficient remained $O(1)$.

3. For the first time two-dimensional retrievals have been obtained from the sharply inhomogeneous absorption distributions over complicated domains, including non-convex ones. In other words, it makes it possible to pose and solve inverse optical problems for translucent media when the sensing radiation is partially screened from the detector.

REFERENCES

1. A.E. Bulyshev, L.G. Velikhanova, and N.G. Preobrazhenskii, *Opt. Spektrosk.* **65**, No. 5, 1139–1144 (1988).
2. V.V. Pikalov and N.G. Preobrazhenskii, *Reconstructive Tomography in Gas Dynamics and Plasma Physics* (Nauka, Novosibirsk, 1987).
3. I.M. Sobol', *Monte Carlo Numerical Methods* (Nauka, Moscow, 1973).
4. V.V. Pikalov and N.G. Preobrazhenskii, *Unstable Problems of Plasma Diagnostics* (Nauka, Novosibirsk, 1982).
5. G.H. Herman, ed., *Image Reconstruction from Projections* (Academic Press, New York, 1980).